Mon. Not. R. Astron. Soc. **000**, ??–?? (2012) Printed 12 December 2012 (MN LATEX style file v2.2)

# A morphological analysis for searches of possible extended $\gamma$-ray sources associated with dark matter annihilation

D. A. Prokhorov[1,2⋆], S. de Jong[3]

[1] *Max-Planck-Institut für Astrophysik, Karl-Schwarzschild-Strasse 1, 85741 Garching, Germany*
[2] *W. W. Hansen Experimental Physics Laboratory, Stanford University, Stanford, CA 94305, USA*
[3] *François Arago Centre, APC, Université Paris Diderot, CNRS/IN2P3, CEA/Irfu, Observatoire de Paris, Sorbonne Paris Cité, 10 rue Alice Domon et Léonie Duquet, 75205 Paris Cedex 13, France*

Accepted ..... Received ..... ; in original form .....

**ABSTRACT**

We propose a morphological analysis for searches of extended $\gamma$-ray emission associated with dark matter annihilation. Our approach is based on the likelihood analysis including the spatial templates produced by taking into account the residual count maps in the energy band in that the dark matter annihilation spectrum has a prominent spectral feature. The approach is tested on the example of the possible dark matter annihilation signal from the Virgo cluster of galaxies.

**Key words:**

## 1 INTRODUCTION

Model selection is an important part of any statistical analysis (Burnham & Anderson 2002). One needs to make assumptions about the pertinence of a model taking into account relevant physical processes. Residual count maps, obtained from the subtraction of the modeled count map (obtained as the result of a likelihood analysis) from the observational data, can contain spatial or spectral structures. These structures are more likely due to imperfections of the selected model rather than the evidence for a new physical process. In this paper, we analyse the data taken by the *Fermi* Large Area Telescope (LAT) from the region including the Virgo cluster of galaxies and propose a method to test the presence of possible extended $\gamma$-ray emission.

A number of astrophysical source classes including supernova remnants (SNRs), pulsar wind nebulae (PWNe), molecular clouds, normal galaxies, and clusters of galaxies are expected to be spatially extended and resolvable by the *Fermi*-LAT. An analysis of extended objects is more complex compared with that of point-like objects because the extension of an object is an additional degree of freedom in the model. The LAT has firmly detected seven SNRs extended at GeV energies, three extended PWN, three nearby galaxies, and the lobes of one radio galaxy, Centaurus A, during the first 2 years of the *Fermi* mission (for a catalog, see Nolan et al. 2012), see also Lande et al. (2012) for observations of other extended objects. Galaxy clusters are promising candidates to $\gamma$-ray emitting sources which can potentially be detected by *Fermi*-LAT (e.g., see Miniati 2003). The mass of galaxy clusters is dominated by dark matter (Zwicky 1933) that is nonbaryonic (for a review, see Bergström 2000). While the nature of dark matter is still unknown, a weakly interacting massive particle (WIMP) is a popular candidate. $\gamma$-ray emission produced through dark matter annihilation may be detectable by *Fermi*-LAT . Thus, galaxy clusters can be diffuse sources associated with dark matter annihilation (e.g., see Ackermann et al. 2010a).

To search for an extended object on the maps of *Fermi*-LAT, one needs to make assumptions about its spatial morphology and spectrum. One of the methods to make such assumptions is to adopt a spatial template associated with emission in a different energy band (e.g. at radio or X-ray frequencies), however this is no guarantee that the spatial morphologies are similar since different radiative processes can give contributions at different frequencies. Another method is to choose the shape of the photon spectrum, e.g. a power-law, but the photon spectrum of a candidate source is *a priori* unknown. The likelihood ratio test allows us to compare candidate models to determine which one gives a better description of the data, but the set of models can never be totally complete and the likelihood ratio test can be applied only for a comparison of nested candidate models.

Residual count maps can be used to produce spatial templates and to determine shapes of spectra for new extended $\gamma$-ray source candidates. This technique can be successfully used if foreground and background emission is perfectly modeled. However, there are some uncertainties in the

⋆ E-mail:phdmitry@gmail.com

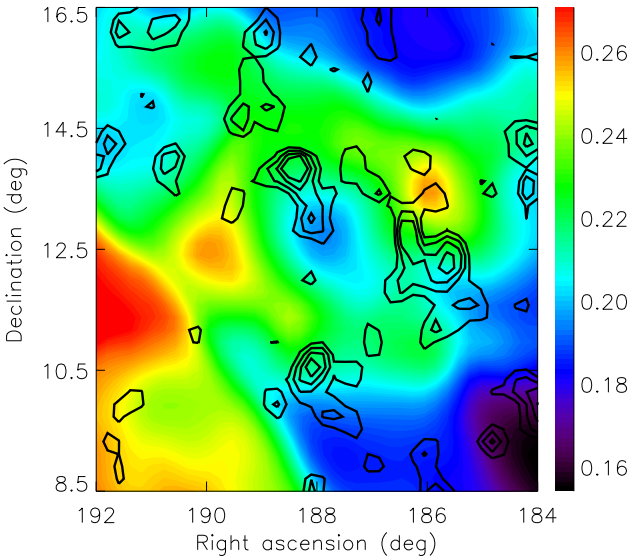


**Figure 1.** The residual count map for the energy range 1-3 GeV is shown by contour lines. The residual map was smoothed with a 2D Gaussian kernel of $\sigma = 0.4°$. The contour levels correspond to 0.6, 1.0, 1.4, and 1.8 counts per pixel.

determination of foreground and background emission. The method that we present below and that will be applied for testing the presence of extended objects is based on the analysis of assumptions on the spectral and spatial properties of an extended object which adopted in the model in which candidates to extended objects are supposed (and their presence is consistent with observations at the high statistical significance). If the modification to the assumptions results in a strong decrease of the statistical significance of a candidate extended object then the model should be reconsidered. Below we demonstrate how to search for the presence of extended emission from the Virgo cluster that could potentially be produced via the annihilation of dark matter particles. The presented method will allow us to study the presence of an extended object associated with the Virgo cluster and can be applied for a search for extended objects associated with high dark matter concentrations, such as the Galactic Center and Andromeda, in the future.

## 2 APPARENT EXTENDED EMISSION FROM THE DARK MATTER HALO IN VIRGO

Clusters of galaxies are the largest gravitationally bound structures in the Universe, with sizes of $\simeq$1-3 Mpc, containing hundreds of galaxies and a hot ($\simeq$1-10 keV) diffuse plasma which sets in equilibrium in the potential wells of the clusters (for a review, see Sarazin 1986). The presence of non-baryonic matter, known as Dark Matter (DM), was inferred from its gravitational effects on visible matter. The DM component contributes $\simeq$80% to the total mass of a galaxy cluster, $M \simeq 10^{14} - 10^{15} M_{\odot}$. The nature of DM remains unknown. Weakly interacting massive particles (WIMPs) are hypothetical particles serving as one possible solution to the dark matter problem and are predicted by many new physics models beyond the standard model of particle physics (for a review, see Bertone et al. 2005). $\gamma$-rays from annihilation of WIMPs in galaxy clusters could potentially be detected by *Fermi*-LAT (for a review of the present status of searches for particle DM by astronomical instruments, see Porter et al. 2011). The search for GeV emission from clusters of galaxies using data collected by the LAT from 2008 August to 2010 February has been reported by Ackermann et al. (2010b), who derived $\gamma$-ray flux upper limits from galaxy clusters under the assumption that galaxy clusters are $\gamma$-rays point-like (i.e., non-extended) sources.

The Virgo cluster is located about 16.5 Mpc away and is the nearest large galaxy cluster. This cluster of galaxies is an excellent target for $\gamma$-ray observations and can spatially be resolved by *Fermi*-LAT at GeV energies because of Virgo's proximity. Recently, a signal consistent with that expected from DM annihilation in the DM halo of the Virgo cluster has been proposed by Han et al. (2012a), who have analyzed the first 3 years of data from *Fermi*-LAT. Note that a large boost factor, $\sim 10^3$, is required for the consistency between the observational data and DM interpretation. The reported signal is at a significant level of $4.4\sigma$ for a model in which WIMPs, with mass $M \simeq 28$GeV, annihilate into the $b\bar{b}$ channel.

As was shown by Macías-Ramírez et al. (2012) and Han et al. (2012b), the tentative evidence for a $\gamma$-ray excess from the Virgo cluster is mainly due to the appearance of a population of $\gamma$-ray point sources with power-law spectra near the Virgo cluster that are not part of the LAT 2-year point source (2FGL) catalog (Nolan et al. 2012). The 2FGL catalog contains significant $\gamma$-ray point sources detected by the LAT in the first 24-months of the *Fermi* mission. The new $\gamma$-ray point sources are found to be above the standard detection significance threshold when more than two years of LAT data is included. The inclusion of the 7 new point sources in the original model of Han et al. (2012a), that are above the test-statistics (Mattox et al. 1996) of TS=25 threshold for the four year data, decreases the significance of the possible DM signal from the $\simeq 5\sigma$ level to $\simeq 3\sigma$ level (Macias-Ramirez et al. 2012).

Note that the presence of the central galaxy of M87, that is also a $\gamma$-ray source, in the Virgo cluster makes the analysis of this cluster more complex, since the subtraction of M87 from the data is necessary for studying the possible extended component associated with the DM halo of the Virgo cluster. The separation of these two $\gamma$-ray emission components can be performed by analysing the emission with energies of $\gtrsim$1 GeV at which the FWHM of the point spread function (PSF) is less than the expected angular size of the DM halo. Annihilation of WIMPs of $M \simeq 28$GeV should produce a $\gamma$-ray signal resulting in an excess at energies of $\simeq$1-3 GeV over the total emission from point sources, diffuse galactic foreground, and isotropic background (this excess should be owing to the specific spectral shape of emission from DM annihilation occured via the $b\bar{b}$ channel, see Sect. 4). The excess of $\gamma$-ray emission from the Virgo cluster at $\simeq$1-3 GeV energies over that expected from 2FGL sources, diffuse galactic foreground, and isotropic background was demonstrated by Han et al. (2012a, see the right panel of their Fig. 12). The presence of the excess in the spectrum leads us to the idea that the analysis of residual count maps at energies of a few GeV can be useful for studying the

morphology of extended emission from the Virgo cluster. In this paper, we will prove the importance of a morphological analysis for the study of extended $\gamma$-ray sources.

## 3 OBSERVATION AND DATA REDUCTION

*Fermi* was launched on 2008 June 11 into a nearly circular Earth orbit with an altitude of 565 km and inclination of 25.6°, and an orbital period of 96 minutes. The principal instrument on *Fermi* is the LAT (Atwood et al. 2009), a pair-production telescope with a large effective area ($\sim$8000 cm$^2$ at 1 GeV) and field of view (2.4 sr), sensitive to $\gamma$-rays between 20 MeV and >300 GeV. After the commissioning phase, the *Fermi*-LAT began routine science operations on 2008 August 4. The *Fermi*-LAT normally operates in sky-survey mode which provides a full-sky coverage every 3 hours (i.e., 2 orbits).

For the data analysis, we use the Fermi Science Tools v9r27p1 package[1] and P7V6 instrument response functions (IRFs). Events $\geqslant$100 MeV arriving within 20° of M87 (region of interest – ROI) and satisfying the SOURCE event selection are taken. To reduce the contamination by the $\gamma$-ray emission coming from cosmic-ray interactions in the Earth's upper atmosphere our selection is refined by choosing events with zenith angles <100°. For this analysis, we have accumulated events obtained from 2008 August 4 to 2012 June 12.

Our aim is to study the morphologies of spatial structures on the residual count map of the Virgo cluster at energies of a few GeV. The residual count map is the result of the subtraction of the modeled count map based on the result of a likelihood analysis from the observational data. To demonstrate the approach for studying extended objects, we include the 2FGL point sources and the diffuse foreground and background in the model as was done by Han et al. (2012a). Our model includes the 2FGL sources located within the ROI. Their spectral shapes are taken from the 2FGL catalog (Nolan et al. 2012), while the normalizations and spectral parameters of sixteen strong point sources (including M87) are derived from the likelihood analysis (the list of the sixteen strong sources are shown in Table 1). The normalizations of fainter point sources are held fixed at the 2FGL catalog values. The galactic diffuse foreground and isotropic diffuse background[2] are included in the model by the templates, gal_2yearp7v6_v0.fits and iso_p7v6source.txt, respectively. The normalizations of the galactic and isotropic components are allowed to vary during the fitting. Note that our model is more realistic than that of Han et al. (2012a), because the parameters of only three 2FGL point sources within the Virgo's virial radius of 4.6° have been allowed to vary in their analysis. As shown in Fig. 1 of Han et al. (2012a), the three point sources within the Virgo's virial radius are faint and, therefore, the residuals are dominated by the contribution from stronger $\gamma$-ray sources which are outside the virial radius. This is because their spectral parameters are not perfectly described by the values taken from the 2FGL catalog, while the data from a longer *Fermi*-LAT observation is analyzed. Since the values of the spectral parameters of the sixteen strong point sources are derived from the likelihood analysis in our study, the calculated residual count maps (see Sect. 4) are more suitable for the morphological analysis than those from Han et al. (2012a). We will discuss a population of $\gamma$-ray point sources near the Virgo cluster (that are not part of the 2FGL catalog) in Sect. 5, where the results of our likelihood analysis will be presented.

**Table 1.** The list of the sixteen strong sources in the ROI

| | |
|---|---|
| 2FGLJ1158.8+0939 | 2FGLJ1204.2+1144 |
| 2FGLJ1209.7+1807 | 2FGLJ1214.6+1309 |
| 2FGLJ1214.8+1653 | 2FGLJ1222.4+0413 |
| 2FGLJ1224.9+2122 | 2FGLJ1229.1+0202 |
| 2FGLJ1230.8+1224 | 2FGLJ1231.6+1417 |
| 2FGLJ1239.5+0443 | 2FGLJ1239.5+0728 |
| 2FGLJ1251.2+1045 | 2FGLJ1256.1-0547 |
| 2FGLJ1301.5+0835 | 2FGLJ1305.0+1152 |

## 4 LIKELIHOOD ANALYSIS AND RESIDUAL COUNT MAP BETWEEN 1 AND 3 GEV

We analyse the first 3.8 years of *Fermi*-LAT observations using the binned maximum likelihood mode of the gtlike routine, which is part of the Science Tools[1]). The test-statistic (TS) (Mattox et al. 1996) was employed to evaluate the significance of the $\gamma$-ray fluxes coming from the sources. The TS value is defined as twice the difference between the log-likelihood function maximized by adjusting all the parameters of the model, with and without the source. The choice of the free and fixed parameters in the analysis is described in Sect. 3. The list of the sixteen 2FGL point sources that spectral parameters were free in the fit is shown in Table 1. We set the energy binning to 30 logarithmic bins between 100 MeV and 300 GeV.

From the resulting best-fit we construct the model counts map in the 1-3 GeV band using the gtmodel tool from the Science Tools. We choose this energy interval because it corresponds to photon energies at which the $\gamma$-ray emission from DM annihilation of WIMPs with $M \simeq 28$ GeV via the $b\bar{b}$ channel should strongly contribute to the total signal (see, e.g., Baltz et al. 2007). Note that the photon spectrum, $dN/dE$, corresponding to annihilation of WIMPs with $M \simeq 25$ GeV via the $b\bar{b}$ channel can be approximated as an exponentially cutoff power-law function with $\Gamma$=1.22 and $E_{\rm cut} = 1.8$ GeV (see, Ackermann et al. 2012)

$$\frac{dN}{dE} = N_0 \left(\frac{E}{E_0}\right)^{-\Gamma} \exp\left(\frac{-E}{E_{\rm cut}}\right), \qquad (1)$$

where $N_0$ and $E_0$ are a prefactor and a scale factor. The value of the exponential cut-off, $E_{\rm cut} = 1.8$ GeV, lies in the energy interval of (1 GeV, 3 GeV) and the spectral index, $\Gamma$, is very hard at energies below the exponential cut-off compared with a typical spectral index of 2FGL point sources. Therefore, the flux excess in the 1-3 GeV energy range can be interpreted as the exponential break in the exponentially-cutoff-power-law spectrum of an additional component produced by DM annihilation. The additional component that could be consistent with possible annihilation emission of DM particles with $M \simeq 28$ GeV was found by Han et al. (2012a) in their likelihood analysis adopting the specific

[1] http://fermi.gsfc.nasa.gov/ssc/data/analysis/
[2] http://fermi.gsfc.nasa.gov/ssc/data/access/lat/BackgroundModels.html

spatial DM template based on high resolution cosmological simulations by Gao et al. (2012), assuming DM annihilation spectra, and including only point sources from the 2FGL catalog in the original model. Therefore, we suppose that this component can potentially also be revealed on the residual count map at 1-3 GeV by studying morphology of residuals.

Figure 1 shows the residual count map of size $8^\circ \times 8^\circ$ (2.3 Mpc×2.3 Mpc) for the energy range 1-3 GeV by contour lines. The pixel size is $0.1^\circ$. This map is derived from the observed LAT count map by subtracting the model obtained from the likelihood analysis and is centered on the position of M87. The residual map was smoothed with a 2D Gaussian kernel of $\sigma = 0.4^\circ$. The contour levels correspond to 0.6, 1.0, 1.4, and 1.8 counts per pixel. The residual count map reveals three prominent structures near the Virgo cluster that have approximate coordinates $\simeq$ (188°, 13.5°), $\simeq$(188°, 10.5°), and $\simeq$(186°, 12°). We also show the galactic diffuse foreground model in the energy band of 1-3 GeV in Fig. 1 by color. The galactic diffuse model is taken from the spatial and spectral template, gal_2yearp7v6_v0.fits, provided by the *Fermi*-LAT collaboration[3]. This model for the Galactic diffuse emission was developed using spectral line surveys of HI and CO (as a tracer of H2) to derive the distribution of interstellar gas in Galactocentric rings. Infrared tracers of dust column density were used to correct column densities in directions where the optical depth of HI was either over- or underestimated. The model of the diffuse $\gamma$-ray emission was constructed by fitting the $\gamma$-ray emissivities of the rings in several energy bands to the LAT observations after removal of the point sources. In the southeastern quadrant of this map, the North Polar spur (the rim of a hot galactic superbubble) is contributing to the foreground galactic diffuse emission model.

In the next section, we attempt to understand the origin of these three prominent structures on the 1-3 GeV residual count map and to discuss whether or not their origin can be caused by DM annihilation emission from the dark matter halo of the Virgo cluster. The aim of the following study is to demonstrate that the residuals at the exponential break energy of the assumed additional spectral component can be used for producing templates and that it is useful to include the spatial templates in the analysis in order to interpret the observations by means of a likelihood analysis.

## 5 LIKELIHOOD ANALYSIS AND MORPHOLOGY OF RESIDUALS

In this Section, we make various spatial templates for the additional $\gamma$-ray component coming from the region of the Virgo cluster. We take the morphology of the residual count map at energies of 1-3 GeV into account and compare the models associated with the spatial templates using the likelihood ratio test for goodness of fit.

The dominant foreground $\gamma$-rays are produced by the neutral pion decay originating from interactions of CR protons with the interstellar medium (ISM). The $\gamma$-ray intensity from neutral pion decay is proportional to the integral along the line of sight of the product of the ISM density and the cosmic ray (CR) proton density. The resulting $\gamma$-ray distribution produced via neutral pion decay should be morphologically correlated with other maps of spatial tracers of the ISM, such as spectral lines of HI and CO, and dust continuum.

Figure 1 shows that the galactic diffuse emission is inhomogeneous in the region of the Virgo cluster and that the galactic diffuse emission map of this region contains the spatial structure that has the shape of a doughnut and that is centered on M87. The three prominent structures on the residual count map at 1-3 GeV lie approximately on this $\gamma$-ray "doughnut" structure (see Fig. 1). To clarify the origin of the "doughnut" structure on the diffuse galactic emission map, we use the HI gas map obtained by the *Leiden/Argentine/Bonn* Survey of Galactic HI Kalberla et al. (2005). We checked and found that the HI map contains a similar "doughnut" structure and that the positions of the HI gas "doughnut" and of the diffuse emission "doughnut" structure are spatially coincident. Therefore, we conclude that the presence of the "doughnut" structure on the galactic diffuse emission map is owing to the particular shape of the HI gas spatial distribution in this region. Note that the residuals in the 1-3 GeV energy band for this $8^\circ \times 8^\circ$ region are highest on the "doughnut" structure and, therefore, the *Fermi*-LAT observations of this region are not described properly by the galactic diffuse template and 2FGL point sources.

### 5.1 Spatial templates

We create the first spatial template, dubbed *doughnut*, taking into account the approximate spatial coincidence of the locations of the foreground emission "doughnut" structure and of the high residuals at 1-3 GeV. This template is shown on the upper left panel in Fig. 2. The radii of the inner and outer circular boundaries of the *doughnut* are $R_{\rm inner} = 1^\circ$ and $R_{\rm outer} = 2.2^\circ$, respectively, and were choosen according to the morphology of the structure on the galactic diffuse emission map shown by color in Fig. 1. The normalization coefficient, $X$, shown on the map, is derived by using the rule, $X = 1{\rm sr}/(\pi R^2_{\rm outer} - \pi R^2_{\rm inner})$. Note that the template, *doughnut*, is homogeneous and, therefore, the possible variations of the gas column density over the HI gas "doughnut" structure are not taken into account.

The second spatial template is associated with the "disk" inside the foreground emission "doughnut" structure in Fig. 1 (i.e., the "disk" corresponds to the hole of the "doughnut"). This template, dubbed *disk*, corresponds to the inner region with a size of $1^\circ$ of the Virgo cluster and is shown on the upper right panel in Fig. 2. The values, $X$, on the map were derived by using the rule, $X = 1{\rm sr}/(\pi R^2_{\rm inner})$. Note that the surface area of the *disk* template is $\approx 3.8$ times smaller than that of the *doughnut* template. The number of *Fermi*-LAT photon events (as well as the incoming photon flux) associated with a spatial template, are proportional to the surface area of a template. Therefore, the DM annihilation signal from the *doughnut* template might be stronger than that from the *disk* template. However, the $\gamma$-ray signal from DM annihilation is proportional to the integral along the line of sight of the squared mass density of dark matter $\int \rho^2_{\rm DM} dl$ and can strongly depend on the spatial

[3] http://fermi.gsfc.nasa.gov/ssc/data/access/lat/Model_details/Pass7_galactic.html

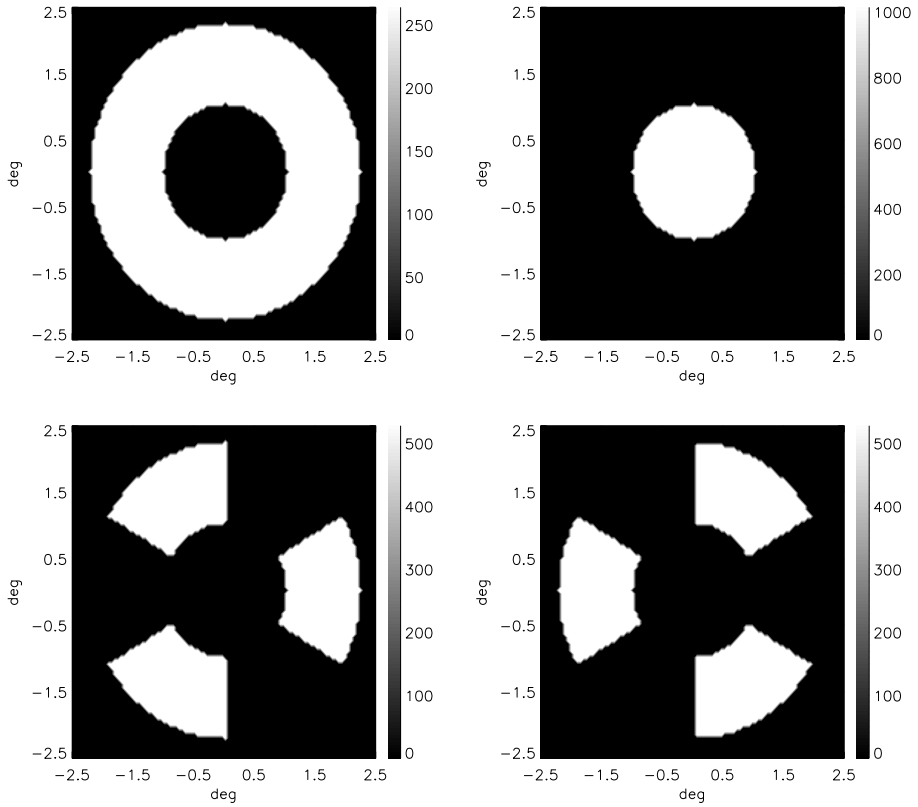


**Figure 2.** Templates which we use for the comparison of different models of the origin of the excess between 1-3 GeV from Virgo

DM distribution (thus, a cusped DM profile can increase the DM annihilation signal from the inner part of the Virgo cluster).

The third and fourth spatial templates (dubbed *petals1* and *petals2* owing to their spatial shapes) are each composed of three distinct parts of equal surface areas. The centers of the three parts belonging to each of these spatial templates are located at the apices of an equilateral triangle. The third and fourth templates are shown on the lower left and lower right panels, respectively, in Fig.2. The values, $X$, on the map were derived by using the rule, $X = 1\mathrm{sr}/(\pi R^2_{\mathrm{outer}}/2 - \pi R^2_{\mathrm{inner}}/2)$. The sum of the third and fourth templates (with equal weighting factors) is identical to the first template, *doughnut*, multiplied by a factor of 2. The template, *petals1*, covers the three prominent structures on the 1-3 GeV residual count map, while the template, *petals2*, does not spatially overlap with these prominent structures on the 1-3 GeV residual map. The DM distribution in the halos of relaxed clusters is expected to be roughly spherically symmetrical and, therefore, the *petals1* and *petals2* templates should be useful to test the possible deviation from the continuous spherical symmetry of the DM distribution. Note that a large part of the mass of the Virgo cluster is centered on the galaxy M87, with smaller concentrations around M86 (at RA$\approx$186.55°, DEC$\approx$12.95°) and M49 (at RA$\approx$187.44°, DEC$\approx$8.00°), see, e.g., Böhringer et al. (1994). The mass concentration around M86 is part of a small group of galaxies that is merging with the main galaxy cluster and is covered by the spatial template *petals2*. Thus, if the DM distribution is the same as described by Böhringer et al. (1994), we expect that the model including the two spatial templates, *disk* and *petals2*, should be the more statistically significant than that includes the spatial template *petals1*.

### 5.2 Morphological analysis

Morphological analysis is a problem-structuring technique of combining parameters into new combinations for the later review. Below we apply the morphological analysis to the study of the *Fermi*-LAT observations of the Virgo cluster in order to show that the residuals at the energy at that the dark matter annihilation spectrum has a prominent spectral feature can be successfully used for the search for extended $\gamma$-ray sources associated with DM annihilation.

We assume the presence of the possible additional components with different spatial distributions, which have not been included in the likelihood analysis in the previous section, and perform a likelihood analysis for various models. The results of likelihood analyses are shown in Table 2. The model, M0, is identical to that considered in the previous section and includes 2FGL sources, galactic foreground, and isotropic background. The model, M1, is nested with the model, M0, and includes the additional template, *doughnut*, with the photon spectrum given by Eq. 1 and mimicking the possible DM annihilation spectrum. The models, M2, M3, M4, are also nested with the model, M0, and include the additional spatial templates, *disk*, *petals1*, and *petals2*, respectively, and their spectral distributions are taken from

Eq. 1. The models, M1, M2, M3, and M4, each include one additional free parameter, compared with the model M0, that corresponds to the normalization of an additional component. The models, M5 and M6, are more complex and include two additional templates, *petals1* + *petals2*, and, *petals2* + *disk*, respectively. The spectral shapes of each of these components are given by Eq.1 and their normalizations are independent free parameters in likelihood analyses. The model, M5, is nested with the models, M0, M1, M3, and M4, whereas the model, M6, is nested with the models, M0, M2, and M4. The calculated log-likelihood values for the described models are shown in the fourth column of Table 2. The difference, multiplied by two, between the log-likelihood function maximized by adjusting all the parameters of the model, with (L) and without ($L_0$) the additional component, are shown in the fifth column of Table 2 (note that the model without any additional component is M0).

The model with an additional component (with free normalization) will always fit at least as well (have a greater log-likelihood) as the model without additional component. Whether it fits significantly better and should thus be preferred is determined by deriving the probability of the difference in the log-likelihoods. Where the null hypothesis represents a special case of the alternative hypothesis (i.e., the case of nested models), the probability distribution of the test statistics is approximately a chi-squared distribution with degrees of freedom equal to $df_2$ - $df_1$, where $df_1$ and $df_2$ represent the number of free parameters of two candidate models. If we take the model, M0, as a null model then using the fifth column of the table we find that the models, M1, M3, and M5, significantly better describe the observational data than the model, M0, does. Comparing the model M1 with M0, we find that the significance of the presence of the DM "doughnut" structure is $3.4\sigma$. Comparing the models M3 and M5 with M0, we find that the presence of the template, *petals1*, strongly improves the fit and its significance is $4.3\sigma$ for the model M3 and is $4.0\sigma$ for the model M5. As for the models M2 and M4, our analysis demonstrates that the inclusion of either *disk* or *petals2* templates do not significantly improve the fit. Therefore, the observational data supports the presence of the spatial structure associated with the template, *petals1*, and has no evidence for the presence of other additional spatial structures with the DM spectrum given by Eq.1.

The models M1 and M5 are nested and their comparison with the observational data permits us to check if the model M5 provides a significantly better fit than the model M1. Since the template for the model M5 is produced by using the high 1-3 GeV residuals, this template is not continuously symmetric with respect to the axis passed through the center of the count map (i.e., the position of M87) along the line of sight (although this template has a discrete rotational symmetry of the 6th order, i.e. rotation by an angle of $360^\circ/6=60^\circ$ does not change the template), while the template for the model M1 is continuously symmetric about this central axis. The comparison of these models is a test of the assumption about the continuously symmetry that has been done by Han et al. (2012a). Twice the difference between the log-likelihood of the models, M1 and M5, is 7.52 (see, the fourth column in Table 2). Therefore, the significance of the improvement of the fit by taking into account the two templates, *petals1* or *petals2*, instead of the template, *doughnut*, is $2.7\sigma$. At $2.7\sigma$ there is only one chance in nearly 150 that a random fluctuation would yield the result. Note that the two sources from a new $\gamma$-ray population of seven point sources, proposed by Macías-Ramírez et al. (2012), and nearest to the center of the Virgo cluster are covered by the spatial template, *petals1*. The coordinates of these two point sources are (RA, DEC)=(188.18, 13.56) and (185.48, 12.04). This shows correspondence between the derived high significance of the spatial structure associated with the template, *petals1*, and the tentative point sources beyond the 2FGL catalog. Although the template, *disk*, covers the central part of the Virgo cluster and that the template, *petals2*, covers the mass concentration around M86, the inclusion of these templates in the analysis (the model M6) does not significantly improve the fit compared with that of the original model M0, see the fifth column of Table2.

**Table 2.** The results of likelihood analyses

| Model | Template | d.o.f. | -log(L) | -2 log($L/L_0$) |
|---|---|---|---|---|
| M0 | - | - | 312042.20 | - |
| M1 | doughnut | 1 | 312036.37 | 11.66 |
| M2 | disk | 1 | 312040.88 | 2.64 |
| M3 | petals1 | 1 | 312032.61 | 19.18 |
| M4 | petals2 | 1 | 312041.35 | 1.7 |
| M5 | petals1+petals2 | 2 | 312032.61 | 19.18 |
| M6 | petals2+disk | 2 | 312040.55 | 3.3 |

Thus, we have demonstrated that the residuals at 1-3 GeV allowed us to create the template, *petals1*, which significantly improves the fit to the data and is not associated with the largest mass concentration. Using a prominent feature of WIMP annihilation spectra and creating the spatial templates (covering the highest residuals in the energy band corresponding to the WIMP annihilation spectral feature), we have shown that the presented morphological analysis is a powerful approach for studying extended $\gamma$-ray sources and their possible association with signals from WIMP annihilation.

## 6 CONCLUSION

In this paper we develop and demonstrate how to apply the morphological analysis for the search for the possible extended gamma-ray sources associated with dark matter annihilation. Our approach is based on an analysis of morphology of residual count maps using spatial templates and taking into account a prominent spectral feature of WIMP annihilation. We chose the photon spectrum produced via annihilation of WIMPs with a mass of 25 GeV as an example, since the possible signals from annihilation of WIMPs with such masses have recently been discussed by Hooper & Linden (2011) and Han et al. (2012a) in their analyses of the *Fermi*-LAT observations.

The *Fermi*-LAT (Atwood et al. 2009) is a pair-production telescope with a large effective area ($\simeq$8000 cm$^2$ at 1 GeV) and field of view (2.4 sr), which is sensitive to $\gamma$-rays between 20 MeV and >300 GeV. The point spread function (PSF) for on-axis $\gamma$-rays has a 68% containment radius of about $3^\circ$ at 100 MeV and $0.04^\circ$ at 100 GeV. The

PSF is about 1° at 1 GeV and *Fermi*-LAT allows us to spatially resolve the nearest clusters of galaxies. The detection of the nearest galaxy clusters, such as Virgo and Coma, is one of goals of the *Fermi* mission. A $\gamma$-ray signal from galaxy clusters can be dominated by photons produced via dark matter annihilation. Other extended $\gamma$-raysources on the sky, that can partially be contributed by WIMP annihilation photons, are the Galactic center and the DM halo of the Andromeda galaxy.

DM particles annihilation in astrophysical sources allows us to perform indirect searches for dark matter. We consider the process $\chi\chi \rightarrow b\bar{b}$, the annihilation of pairs of dark matter particles to pairs of b quarks. Spectrum of photons from hadronic processes has a peak which occurs at an energy of $E_{\rm peak} \approx m_{\chi}/25$ (e.g., see Baltz et al. 2007). If a dark matter particle mass is 25 GeV, then we expect the peak in the photon spectrum at $\simeq$ 1 GeV. Therefore, the residual count map at the peak energy, that is produced by the subtraction of the model (without the inclusion of a WIMP annihilation source) from the observational data, could give important information about the morphology of a possible WIMP annihilation source. Note that point like $\gamma$-ray sources with hard spectra at low energies and with a spectral exponential cut-off at a high energy equally well describe pulsar and WIMP annihilation spectra in $\gamma$-rays. Therefore, the extended $\gamma$-ray sources associated with a high concentration of DM provide us with a unique possibility to search for WIMP annihilation $\gamma$-ray signals.

We applied a morphological analysis to the study of the Virgo cluster initially assuming the presence of 2FGL sources, galactic diffuse foreground, and extragalactic diffuse background. We derived the 1-3 GeV residual count map and found that the high residuals at 1-3 GeV are confined in three spatial regions, and that the morphology of residuals is clumpy rather than continuously spherically symmetric. We performed a likelihood analysis using different spatial templates, dubbed *doughnut, disk, petals1, and petals2*, obtained by taking into account the morphology of the high 1-3 GeV residuals. Our analysis demonstrates that the presence of the template, *petals1*, covering the high 1-3 GeV residuals and having the photon spectrum provided by WIMP annihilation, strongly improves the fit and its significance is $4.3\sigma$. The template, *doughnut*, is continuously spherically symmetric, spatially covers the high 1-3 GeV residuals, and its surface is two times larger than the surface of a *petals1* template. The significance of the improvement of the fit by taking into account the two templates, petals1 or petals2, (with equal surface areas) instead of the continuously symmetric template, *doughnut*, is $2.7\sigma$. This shows that the signal which could be associated with WIMP annihilation is not continuously symmetric in the inner part of the Virgo cluster. Therefore, the morphology of residuals at the energy peak of photon spectra corresponding to those of WIMP annihilation is an interesting diagnostics of a dark matter distribution. Studying of the morphology of residual count maps at such energies can be used for a search for extended $\gamma$-ray signals from WIMP annihilation.

## REFERENCES


Ackermann M. et al., 2010a, JCAP, 5, 25
Ackermann M. et al., 2010b, ApJ, 717, L71
Ackermann M. et al., 2012, ApJ, 747, 121
Atwood W. B. et al., 2009, ApJ, 697, 1071
Baltz E. A., Taylor J. E., Wai L. L., 2007, ApJ, 659, L125
Bergström L., 2000, Reports on Progress in Physics, 63, 793
Bertone G., Hooper D., Silk J., 2005, Phys. Rep., 405, 279
Böhringer H., Briel U. G., Schwarz R. A., Voges W., Hartner G., Trümper J., 1994, Nature, 368, 828
Burnham K. P., Anderson D. R., 2002, Model Selection and Multimodel Inference: A Practical Information-Theoretic Approach, Springer, 2002, 488 p. ISBN 0-387-95364-7
Gao L., Frenk C. S., Jenkins A., Springel V., White S. D. M., 2012, MNRAS, 419, 1721
Han J., Frenk C. S., Eke V. R., Gao L., White S. D. M., 2012a, ArXiv e-prints 1201.1003
Han J., Frenk C. S., Eke V. R., Gao L., White S. D. M., Boyarsky A., Malyshev D., Ruchayskiy O., 2012b, ArXiv e-prints 1207.6749
Hooper D., Linden T., 2011, Phys. Rev. D., 84, 123005
Kalberla P. M. W., Burton W. B., Hartmann D., Arnal E. M., Bajaja E., Morras R., Pöppel W. G. L., 2005, A&A, 440, 775
Lande J. et al., 2012, ApJ, 756, 5
Macías-Ramírez O., Gordon C., Brown A. M., Adams J., 2012, Phys. Rev. D., 86, 076004
Mattox J. R., et al., 1996, ApJ, 461, 396
Miniati F., 2003, MNRAS, 342, 1009
Nolan P. L. et al., 2012, ApJS, 199, 31
Porter T. A., Johnson R. P., Graham P. W., 2011, ARA&A, 49, 155
Sarazin C. L., 1986, Reviews of Modern Physics, 58, 1
Zwicky F., 1933, Helvetica Physica Acta, 6, 110